# Please Read the Abstract

By

Abstract Writer

Submitted to the graduate degree program in Department of People who read Abstracts and the Graduate Faculty of the University of Kansas in partial fulfillment of the requirements for the degree of Doctor of Philosophy.

Committee members

MEMBER 1, Chairperson

MEMBER 2, Occasional Visitor

MEMBER 3

MEMBER 4, The One Who Never Answers Email

The One with an Extra Long Name

The Fifth Beatle

Date defended: October 02, 2016

The Thesis Committee for Abstract Writer certifies
that this is the approved version of the following thesis :

Please Read the Abstract

MEMBER 1, Chairperson

Date approved: October 06, 2016

# Abstract

The diffractive dijet photoproduction can probe the nuclear parton distribution at low Bjorken-x.

# Acknowledgements

Thanks to my family and friends.

# Contents

# List of Figures

# List of Tables

# Chapter 1

# Nuclear Physics in Ultra-relativistic Heavy-Ion Collisions

## 1.1 The Standard Model

The Standard Model describes the fundamental particles of the universe in terms of fermions and bosons. Fermions are particles with half-integer spin, while bosons have integer-spin. This difference in spin has far reaching consequences. Fermions must obey the Pauli Exclusion Principle: only one fermion at a time can occupy a given state. However, multiple bosons can simultaneously occupy a specific state.

Among the fermions are the leptons, neutrinos, and quarks. The leptons consist of the electron, muon, and tau, as well as their anti-particles. The leptons are seemingly fundamental: high energy experiments have yet to observe internal lepton-structure. Neutrinos are weakly interacting particles detected primarily through the precise measuring of missing transverse energy in the products of particle collisions. Quarks are the constituent particles of baryons, which contain three valence quarks, and mesons, which contain two valence quarks. In addition to the valence quarks are the sea quarks, which appear and disappear as quark-antiquark pairs within hadrons. The hadrons are particles made of quarks and gluons.

The behavior of fundamental particles is best described within the framework of quantum field theory (QTF). QFT defines a Lagrangian for fundamental particles. This Lagrangian then predicts the outcome of particle collisions. Different terms in the Lagrangian correspond to the various interactions between particles. The Standard Model Lagrangian can be broken down into four basic terms:

$$\mathscr{L}_{StandardModel} = \mathscr{L}_{QED} + \mathscr{L}_{QCD} + \mathscr{L}_{Higgs} + ... \tag{1.1}$$

The QED and QCD Lagrangians will be the most important in what follows. Feynman rules are derived from the Langrangian. Particularly important for the Feynman rules are the coupling constants for the electromagnetic force and strong-nuclear force.

### 1.1.1 Quantum Electrodynamics

Quantum electrodynamics (QED) is a theory of electromagnetic interaction in terms of relativistic quantum field theory. QED addresses three specific processes: photon motion, electron motion, and the emission, or absorption, of a photon by an electron.

The QED coupling decreases with distance, as manifest the Coulomb force being proportional to an inverse-square law.

$$\alpha_{QED}(Q^2) = \frac{\alpha_{em}}{(1 - \frac{\alpha_{em}}{3\pi})\ln(\frac{Q^2}{m^2})} \tag{1.2}$$

### 1.1.2 Quantum Chromodynamics

The quarks are a family of fermions that compose the baryons and the mesons. Baryons consist of three quarks in a color neutral state, while mesons consist two quarks in a color neutral state. "Color" in this context refers to the six kinds of strongly-interacting charge available to quarks: red and anti-red, blue and anti-blue, and green and anti-green. Color charge has no relation to optical phenomena, but provides a useful analogy for the stable combinations of quarks. The net color-charge of a baryon or meson is "white".

Unlike QED, the QCD coupling increases with distance. This has the practical consequence of the strong-interactions being stronger in high momentum transfer collisions. The direct results of the running QCD coupling are the dual phenomena of asymptotic freedom and color confinement. At large distances, string tension describes the binding force of the quarks. At short distances,

however, Coulomb-like interactions dominate.

Within the nucleus, a proton can be thought of as a bubble in a vacuum. Debrye screening exerts a pressure on the proton. This pressure is responsible for the size of the proton.

$$\alpha_{QCD}(Q^2) = \alpha_s(Q^2) = \frac{4\pi}{(11 - \frac{2}{3}n_f)\ln(\frac{Q^2}{\Lambda^2_{QCD}})} \tag{1.3}$$

## 1.2 QCD Experiments

Scattering experiments are the basic tool for exploring the nucleus. The Large Hadron Collider (LHC) is capable of reaching heavy-ion collision energies of up to 7 TeV per nucleon-nucleon. The higher the energy, the more experiments can probe the nuclear phase-space diagram.

At the turn of the century, Ernst Rutherford probed the gold atom by bombarding a gold sheet with alpha-particles (helium nuclei). The angular distribution of the scattered alpha-particles demonstrates that the mass of the atom is concentrated in a small volume, i.e, the atom is mostly empty space.

Momentum transferred, expressed as $Q^2$, is an important quantity for characterizing QCD measurements.

In addition to $Q^2$, Bjorken-x, also known as Bjorken-scaling is necessary to describe the nuclear phase space. Bjorken-x represents the momentum fraction of partons.

### 1.2.1 Hard Processes

Hard processes involve scattering particles off partons in the manner of point-like charges.

#### 1.2.1.1 Deep Inelastic Scattering

Deep inelastic scattering commonly refers to the scattering of a leptons off hadrons. These experiments provided the first evidence of Bjorken-scaling in the nucleus, a direct interpretation of which is the existence of quarks as point-like particles at high energies.

### 1.2.2 Soft Processes

Soft processes compose the low momentum transfer, typically gluon-gluon interactions during a collision.

### 1.2.3 Heavy-Ion Collisions

Similar to the Rutherford experiment, in heavy-ion collisions the scattered particles carry information about the internal structure of the nucleus.

The Rutherford experiment has the three components that still characterize high-energy nuclear experiments: a probe, a medium, and a signal. Alpha particles probe the medium of the gold atom, and the angular distribution of scattered alpha particles signals the internal structure of the atom.

#### 1.2.3.1 Ultra-peripheral Collisions

Ultra-peripheral collisions occur at impact parameters greater than the sum of the heavy-ion radii. In these collisions, hadronic interactions are strongly suppressed while photonuclear activity is enhanced proportional to the square of the nuclear charge. The electromagnetic field of an incoming heavy-ion, from the perspective of a target, is equivalent to a flux of virtual photons.

## 1.3 Jet Production

Gluons are the particle exchanged in strong interactions. However, gluons themselves carry color charge. By analogy, photons transmit the electromagnetic force, but do not themselves have an electric charge.

When a quark is scattered from a nucleus, the strong interaction gathers potential energy until the threshold for quark production is passed, at which point an anti-quark is generated to screen the ejected quark.

### 1.3.1 Diffraction

QCD factorisation describes the diffractive-photoproduction dijet cross-section as the convolution of the partonic cross-section with the diffractive parton distributions. However, factorisation only describes H1 data if the resolved-photon contribution is suppressed.

### 1.3.2 Photoproduction

The photoproduction cross-section is proportional to the gluon distribution.

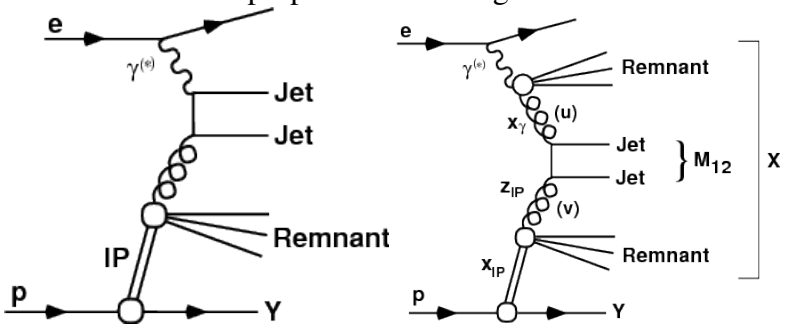


#### 1.3.2.1 Direct Photon Processes

At low momentum transfer, photons interact electromagnetically, i.e. directly, with partons.

#### 1.3.2.2 Resolved Photon Processes

High energy photons possess a hadronic structure.

# Chapter 2

# Diffractive Dijet Photoproduction

Diffractive dijet photoproduction is a powerful constraint on the relationship between next-to-leading order (NLO) and non-perturbative (NP) QCD.

## 2.1 Diffraction in Photon-Hadron Collisions

The DESY collaboration is responsible for measuring the structure functions of the proton via diffraction.

### 2.1.1 Exclusivity

## 2.2 Next to Leading Order QCD + NPDF

## 2.3 Perturbative QCD

At low Bjorken-x, gluon interactions dominate the nucleus. As such, NLO-QCD no longer describes the PDF.

## 2.4 Factorisation Breaking

# Chapter 3

# The Experiment

## 3.1 Large Hadron Collider

The Large Hadron Collider (LHC) has a radius of approximately 27 kilometers. As of this writing, it is the largest machine ever constructed. The initial purpose of the LHC was to discover the Higgs boson, but it is capable of investigating a variety of other physics phenomena, such as dark matter, extra-dimensions, and heavy-ion physics.

LHC is a hadron collider, meaning it is designed to collide particles made of quarks and gluons. The proton-proton, proton-Pb, and Pb-Pb collision energies are the largest ever probed experimentally.

## 3.2 Compact Muon Solenoid

The Compact Muon Solenoid (CMS) is a general-purpose particle detector located at Point-5 of the LHC. CMS was designed to precisely measure the momentum of muons. The titular superconducting solenoid magnet generates a 4 Tesla field. This field is homogeneous and parallel to the beam line close to the interaction point. The momentum of a muon is measured from how it deflects when moving through the magnetic field.

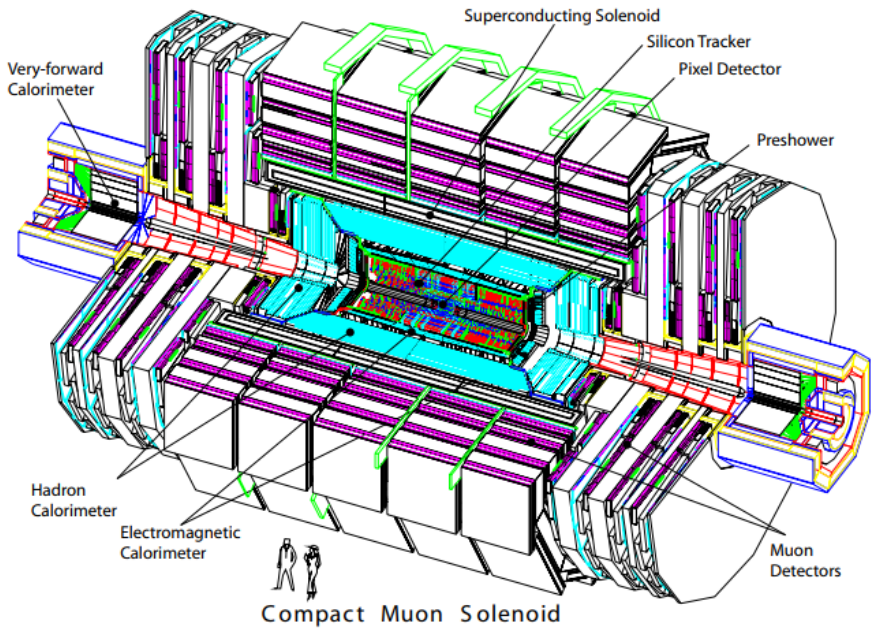


The central feature of the CMS apparatus is a superconducting solenoid of 6 m internal diameter, providing a magnetic field of 3.8 T. Within the solenoid volume are a silicon pixel and strip tracker, a lead tungsten crystal electromagnetic calorimeter (ECAL), and a brass and scintillator hadron calorimeter (HCAL), each composed of a barrel and two endcap sections. The silicon tracker measures charged particles within the pseudorapidity range $|\eta| < 2.5$ . It consists of 1440 silicon pixel and 15 148 silicon strip detector modules and is located in the 3.8 $T$ field of the superconducting solenoid. For non-isolated particles of $1 < pt < 10GeV$ and $|\eta| < 1.4$, the track resolutions are typically 1.5 percent in $pt$ and 25–90 (45–150)$\mu$ in the transverse (longitudinal) impact parameter cite (Chatrchyan:2014fea).

The pseudorapidity coverage for the ECAL and HCAL detectors is $|\eta| < 3.0$. The ECAL provides coverage in the pseudorapidity range $y < 1.5$ in the barrel region (EB) and $1.5 < y < 3.0$ in the two endcap regions (EE). The HCAL provides coverage for $y < 1.3$ in the barrel region (HB) and $1.3 < y < 3.0$ in the two endcap regions (HE). The Hadronic Forward (HF) calorimeters ($3.0 < |\eta| < 5.2$) complement the coverage provided by the barrel and endcap detectors. The zero degree calorimeters (ZDCs) are two Cherenkov calorimeters composed of alternating layers of tungsten and quartz fibers, and situated between the two proton beam lines at above $|\eta| > 8.3$

from the interaction point. The HF and ZDC systems each consist of two detectors on either side of the interaction point: $HF^{+-}$, and $ZDC^{+-}$, respectively. The CASTOR calorimeter is located at a distance of 14.2 m from the interaction point at a radial distance from the LHC beam of about 4 to 15 cm. This corresponds to a pseudorapidty coverage of -6.6 $< y <$ -5.2. A more detailed description of the CMS detector, together with a definition of the coordinate system used and the relevant kinematic variables, can be found in cite(Chatrchyan:2008aa).

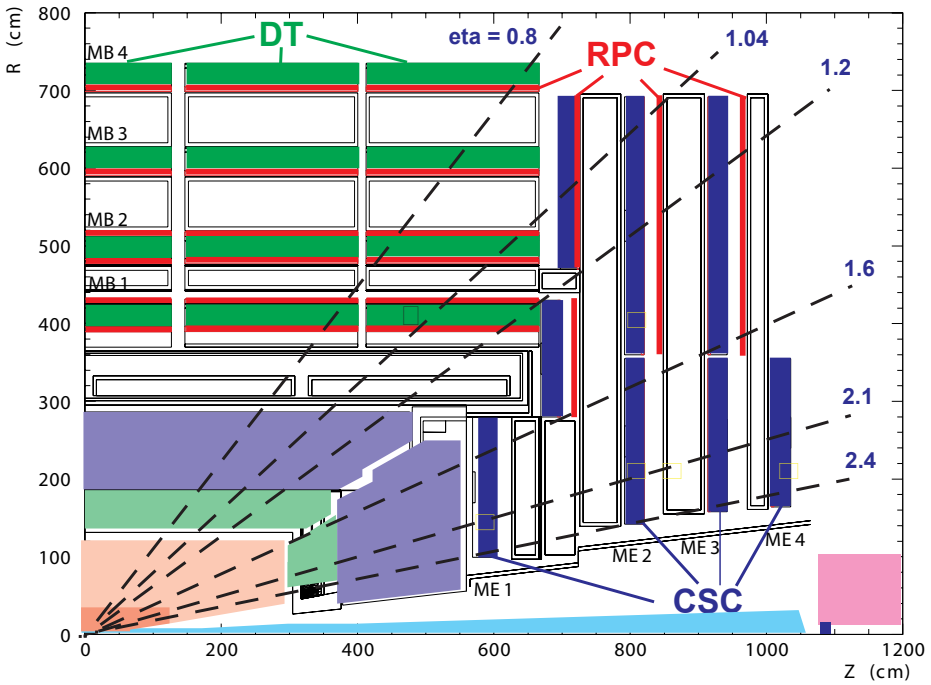


### 3.2.1 Inner Tracker

The tracker measures the momentum of charged particles via their trajectory through a homogenous magnetic field. The tracker consists of two units, the pixel tracker and the strip tracker, both of which are made of silicon. A charged particle causes an electrical signal when passing through a silicon pixel or silicon microstrip. CMS reconstructs these electrical signals, taken at specific points of position and time, into tracks. These tracks are accurate to the 10 micrometers. The tracker is meant to have a particle pass all the way through it, with only minimal effect particle's trajectory.

#### 3.2.1.1 Pixel Tracker

Every silicon-pixel has a corresponding readout chip. The readout chips are soldered through the bump-bonding method. The readout chip amplifies signals from the pixel.

The pixel tracker is precise enough to distinguish the vertices of tracks originating from short-lived particles, such as bottomonia.

#### 3.2.1.2 Strip Tracker

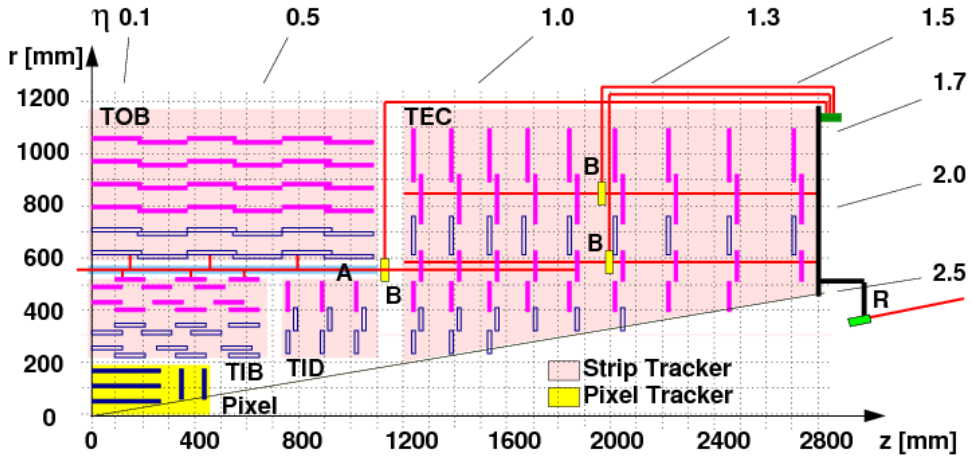


### 3.2.2 Electromagnetic Calorimeter

The Electromagnetic Calorimeter (ECAL) is the dedicated CMS calorimeter for detecting electrons and photons. The calorimeter is comprised of lead tungstate ($PbWO_4$) crystals arranged in cylinder about the beam, including two endcaps. The granularity of these crystals gives the ECAL excellent energy resolution, angular resolution, and spatial resolution. The ECAL is hermetic and homogenous. The data readout is fast enough that CMS can trigger off signals in the ECAL.

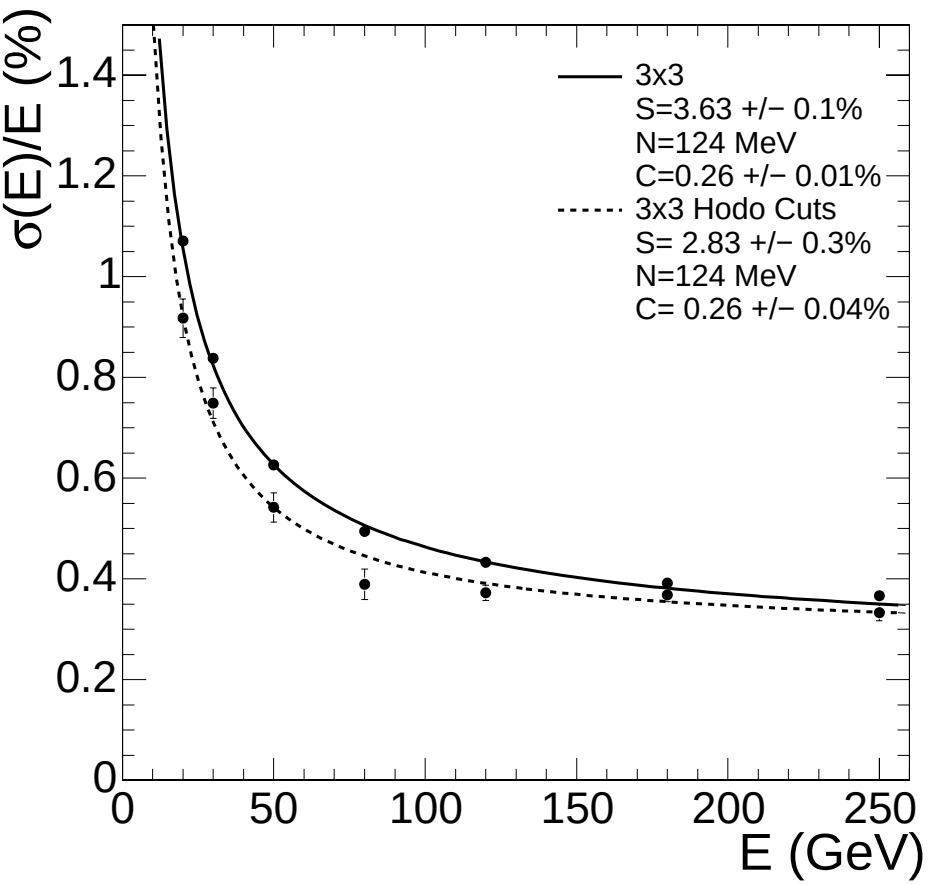


### 3.2.3 Hadronic Calorimeter

The Hadronic Calorimeter (HCAL) has such a large acceptance that it can indirectly observe non-interacting particles such as neutrinos.

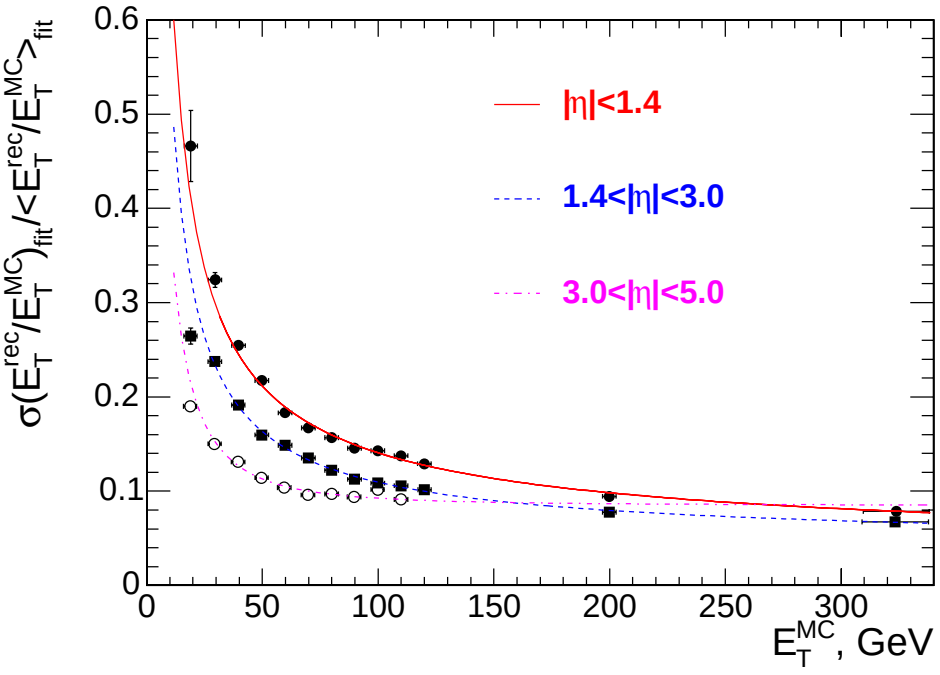


#### 3.2.3.1 Hadronic Forward Calorimeters

The Hadronic Forward Calorimeters (HF) absorbs the greatest portion of energy from collisions. As such it is designed for maximum radiative resistance.

### 3.2.4 Muon Detector

### 3.2.5 Zero Degree Calorimeter

### 3.2.6 Particle Flow Algorithm

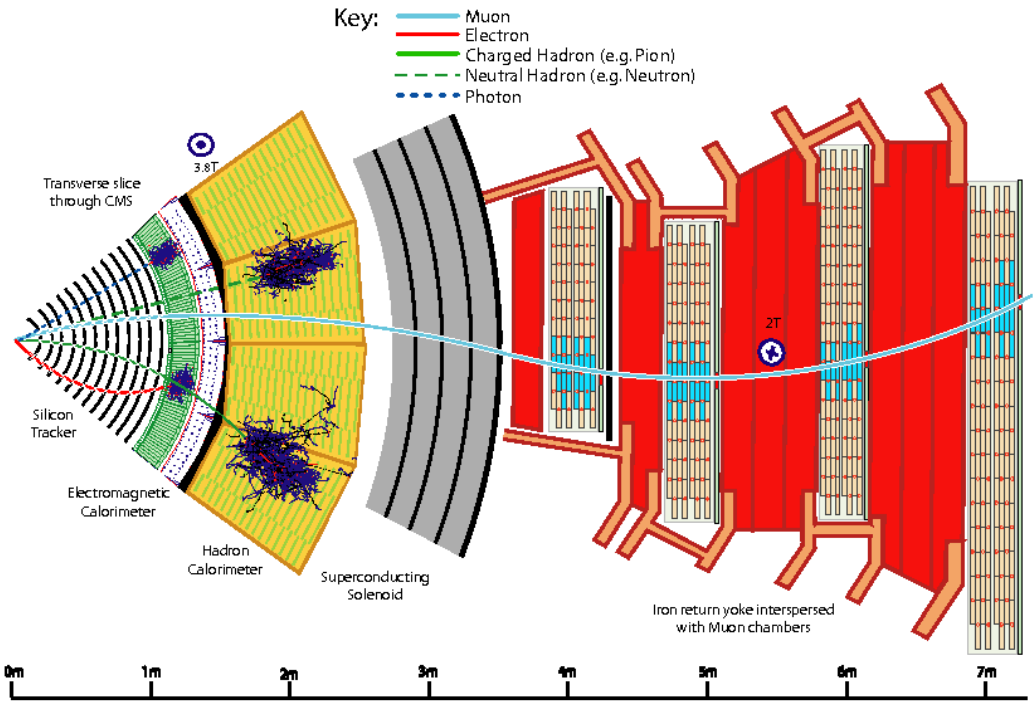


### 3.2.7 Luminosity

One of the most important quantities measured by CMS is luminosity. Luminosity is necessary to convert the number of events detected, for a given channel, into a collision cross-section. Collision cross-sections are among the primary observables predicted by theoretical physics, specifically quantum field theory.

#### 3.2.7.1 van de Meer Scanning

### 3.2.8 Triggering

CMS reconstruct events faster than they can be stored on hard-drives. To account for this phenomena – pile-up – CMS uses a two tiered triggering system. L1 triggers are always online, and for

those events that pass the L1 triggers, the High Level Triggers (HLTs) will select which events are stored as data.

# Chapter 4

# Detecting Photoproduction in Ultra-Peripheral HI Collisions

Central heavy-ion collisions produce large numbers of tracks compared to proton collisions. However, ultra-peripheral collisions are characterized by emptiness in most of CMS. As such, ultra-peripheral collisions can be thought of as the complement to the high multiplicity, hadronically dominated heavy-ion collisions.

## 4.1 Selection on Hadronic Forward Calorimeter

The operative variable for the HF is the maximum calorimeter-tower energy.

## 4.2 Selection on Zero Degree Calorimeter

The zero degree calorimeter detects any neutrons emitted from the colliding nuclei. Neutron emission indicates that the nucleus dissociated, and that the interaction was not coherent. Removing these obviously incoherent events from our data sample improves our signal.

## 4.3 Selection on Pixel Tracker

High purity tracks are recorded by the pixel tracker. These tracks are then used to determine the size of rapidity gaps.

# Chapter 5

# DDPP at DESY

## 5.1 H1

The H1 Collaboration is an experiment hosted by the HERA electron-proton collider at DESY in Hamburg, Germany.

### 5.1.1 Diffractive Jets in ep

Diffractive jet analyses at H1 demonstrate factorization breaking in the nuclear parton distribution. In comparison to H1 data, next-to-leading order QCD calculations of the diffractive-photoproduction dijet cross-section are a factor of two larger than measured.

## 5.2 RAPGAP

RAPGAP is a Monte Carlo generator created for H1 analyses, specifically diffractive studies. By default, RAPGAP models electron-proton and proton-proton collisions. However, ultra-peripheral heavy-ion collisions are distinct from electron-proton collisions only in the photon spectrum. Re-weighing RAPGAP events by the heavy-ion photon spectrum can thus model heavy-ion UPC.

# Chapter 6

# DDPP measurement in CMS forward region

## 6.1 Rapidity Gap

## 6.2 Forward Tagging

## 6.3 Jet Reconstruction

## 6.4 PYTHIA and STARLIGHT

# Chapter 7

# Probing low-x nuclear PDFs with diffractive photoproduction at CMS

The Bjorken-x value of a parton is the fraction of the total nuclei's momentum carried by said parton. The scaling behavior of Bjorken-x proved that the constituents of the nucleus, the partons, are themselves pointlike.

## 7.1 The Probe

Ultra-peripheral collisions are charactered by photoproduction. The photon enters the nucleus and strikes a parton. The resulting dijet carries information about the elliptic gluon distribution in the angular correlation of the dijets.

# Chapter 8

# Conclusions

# References


Aaron, F. D. et al. (2010). Diffractive Dijet Photoproduction in ep Collisions at HERA. *Eur. Phys. J.*, C70, 15–37.

Aaron, F. D. et al. (2011). Measurement of the cross section for diffractive deep-inelastic scattering with a leading proton at HERA. *Eur. Phys. J.*, C71, 1578.

Andreev, V. et al. (2015). Diffractive Dijet Production with a Leading Proton in $ep$ Collisions at HERA. *JHEP*, 05, 056.

Chekanov, S. et al. (2009). Deep inelastic scattering with leading protons or large rapidity gaps at HERA. *Nucl. Phys.*, B816, 1–61.

Crittenden, J. A. (1997). Exclusive production of neutral vector mesons at the electron - proton collider HERA.

Guzey, V. & Klasen, M. (2016a). A fresh look at factorization breaking in diffractive photoproduction of dijets at HERA at next-to-leading order QCD. *Eur. Phys. J.*, C76(8), 467.

Guzey, V. & Klasen, M. (2016b). Diffractive dijet photoproduction in ultraperipheral collisions at the LHC in next-to-leading order QCD. *JHEP*, 04, 158.

# Appendix A

# My Appendix, Next to my Spleen

There could be lots of stuff here